Supporting Information

Coordination Engineering of Ru-N-C Based OER Catalysts Guided by the ΔG_{*OH} Descriptor: A Theoretical Study

Xiaoming Zhang[a], Suli Wang[a,b*], Shansheng Yu[c], Gongquan Sun[a*]

[a]*Division of Fuel Cells and Battery, Dalian National Laboratory for Clean Energy, Dalian Institute of Chemical Physics, Chinese Academy of Sciences, Dalian 116023, China.*
[b]*State Key Laboratory of Catalysis, Dalian Institute of Chemical Physics, Chinese Academy of Sciences, Dalian 116023, China.*
[c]*Department of Materials Science, Jilin University, Changchun 130012, China*

Keywords: *Ru-N-C, OER, Coordination Engineering, DFT*

* Corresponding author.
E-mail addresses: suliwang@dicp.ac.cn (S. L. Wang), gqsun@dicp.ac.cn (G. Q. Sun).

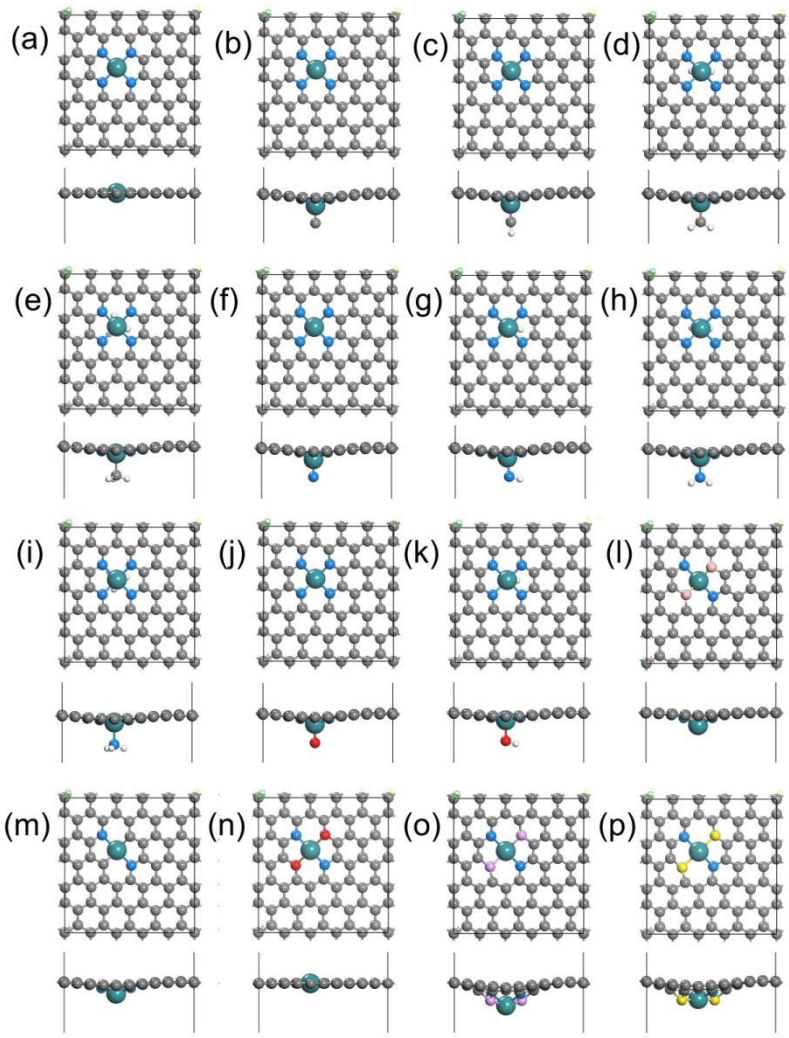

Figure S1. The optimized structures of (a) Ru-N_4-C_{10}, (b) Ru-N_4-C_{10}, (c) Ru-N_4CH-C_{10}, (d) Ru-N_4CH_2-C_{10}, (e) Ru-N_4CH_3-C_{10}, (f) Ru-N_4N-C_{10}, (g) Ru-N_4NH-C_{10}, (h) Ru-N_4NH_2-C_{10}, (i) Ru-N_4NH_3-C_{10}, (j) Ru-N_4O-C_{10}, (k) Ru-N_4OH-C_{10}, (l) Ru-N_2B_2-C_{10}, (m) Ru-N_2C_2-C_{10}, (n) Ru-N_2O_2-C_{10}, (o) Ru-N_2P_2-C_{10}, (p) Ru-N_2S_2-C_{10}.

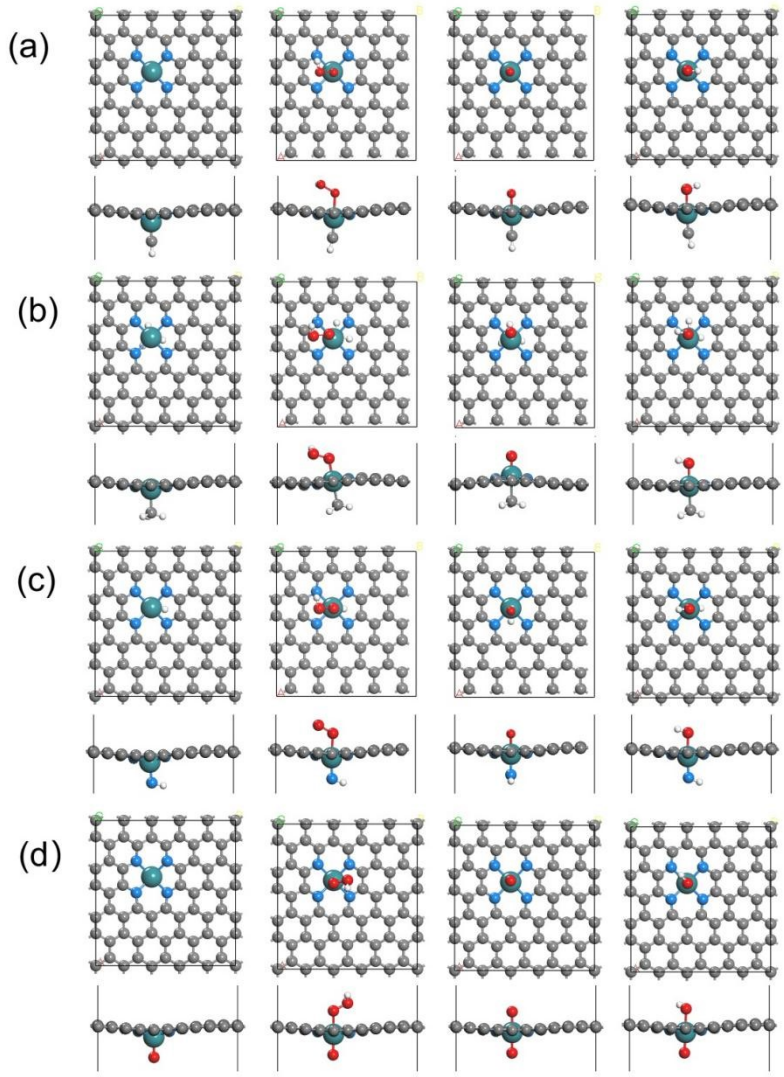

Figure S2 The optimized structures of *OOH, *O and *OH on (a) Ru-N_4CH-C_{10}, (b) Ru-N_4CH_3-C_{10}, (c) Ru-N_4NH-C_{10}, (d) Ru-N_4O-C_{10}.

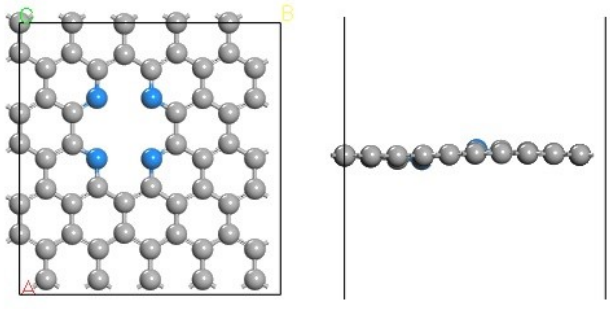

Figure S3 The optimized structures of N doped Graphene.

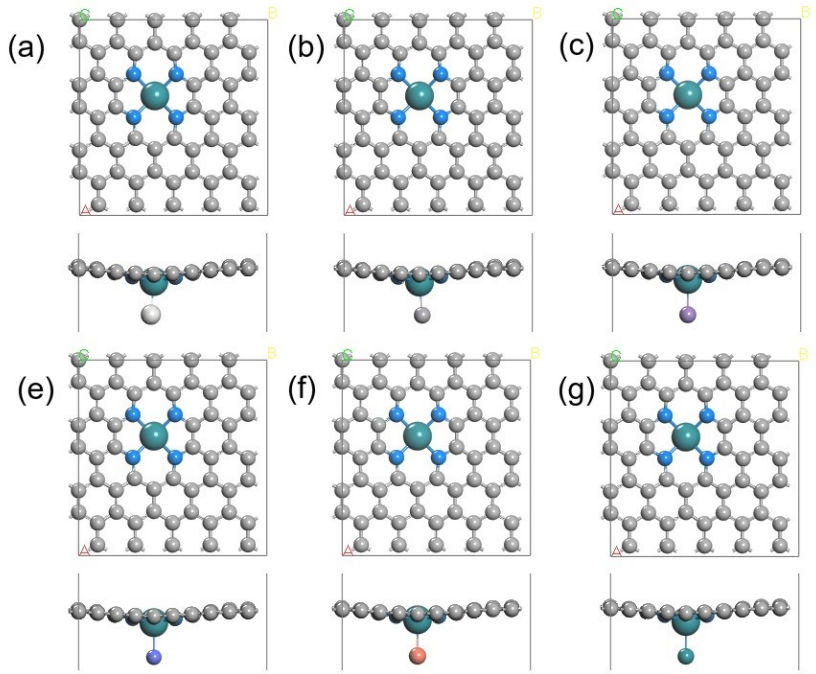

Figure S4 The optimized structures of (a) Ru-N_4Sc-C_{10}, (b) Ru-N_4V-C_{10}, (c) Ru-N_4Mn-C_{10}, (d) Ru-N_4Co-C_{10}, (d) Ru-N_4Cu-C_{10}, (d) Ru-N_4Ru-C_{10}.

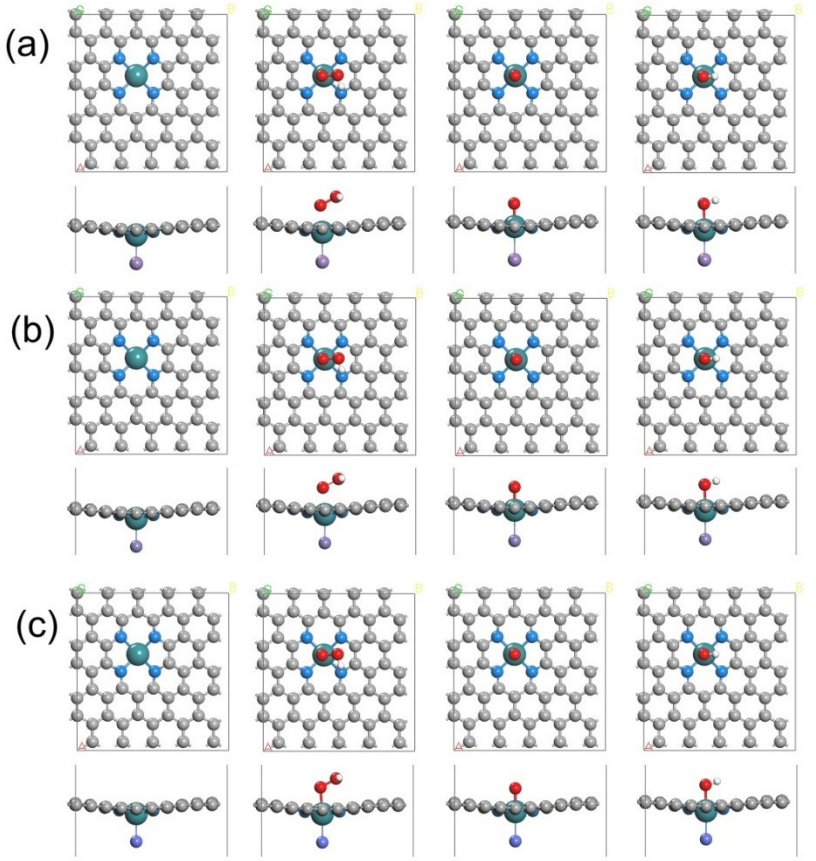

Figure S5 The optimized structures of *OOH, *O and *OH on (a) Ru-N_4Mn-C_{10}, (b) Ru-N_4Fe-C_{10}, (c) Ru-N_4Co-C_{10}.

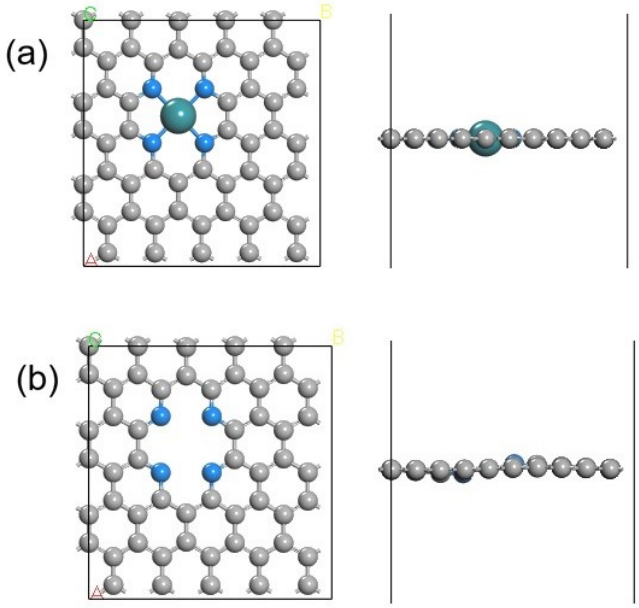

Figure S6 The optimized structures of (a) Ru-N_4M-C_{10} with removed M, (b) N doped Graphene

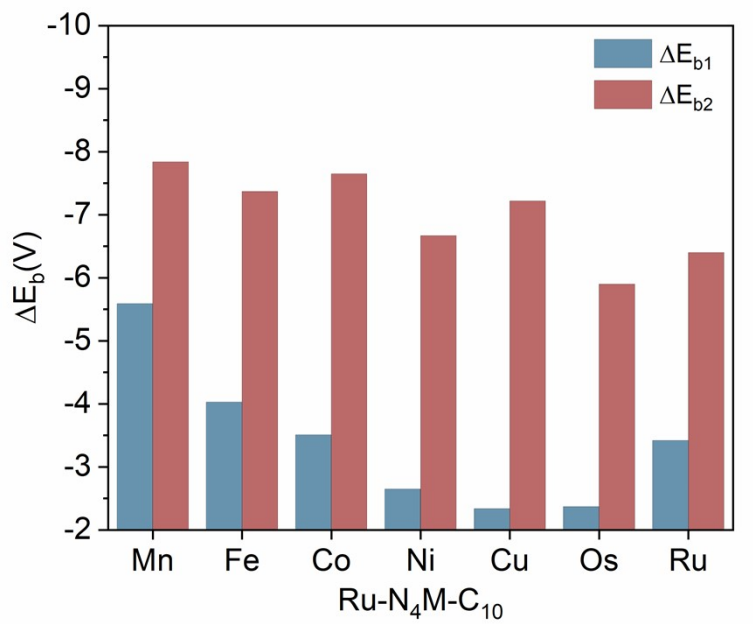

Figure S7 The binding energy comparison of Rh-N_4M-C_{10} OER (M=Mn, Fe, Co, Ni, Cu, Os, Ru) catalysts.

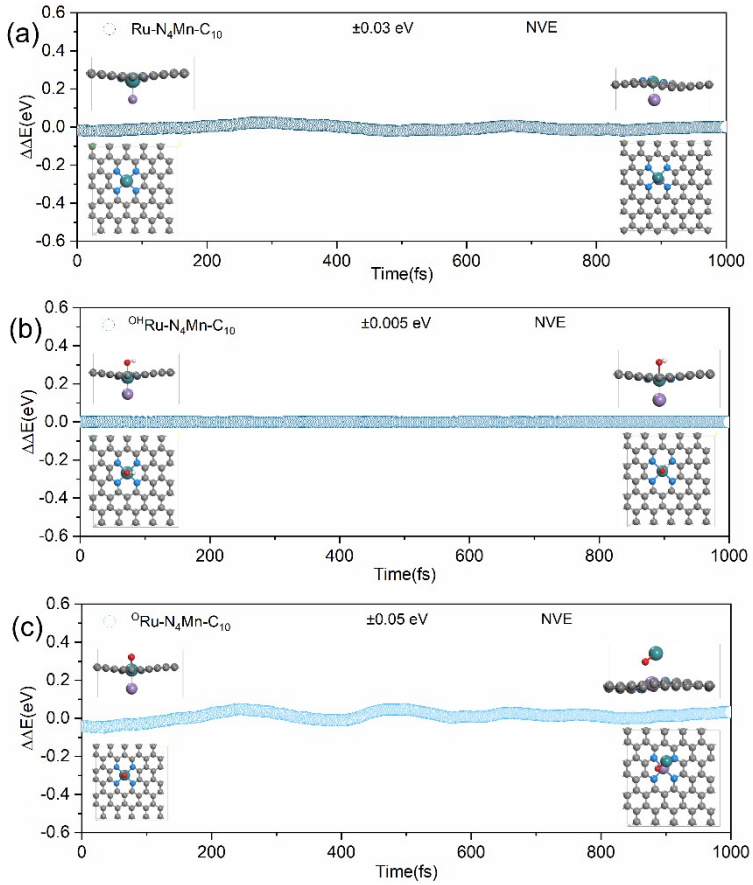

Figure S8. Dynamic stability of (a) Ru-N_4Mn-C_{10}, (b) ^{OH}Ru-N_4Mn-C_{10} and (c) ^{O}Ru-N_4Mn-C_{10} from AIMD simulations

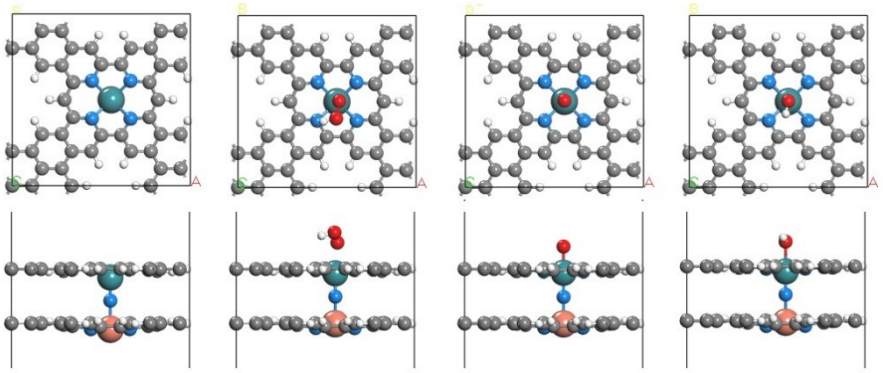

Figure S9 The optimized structures of *OOH, *O and *OH on Ru-CuN_4-C_{10}.

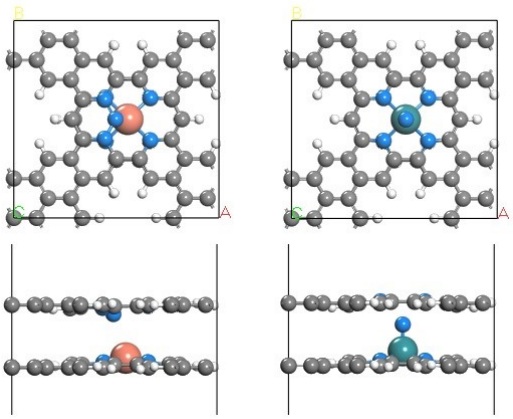

Figure S10 The optimized structures of (a) Ru-CuN_4M-C_{10} and (b) Ru-CuN_4M-$C_{10}$with removed Ru

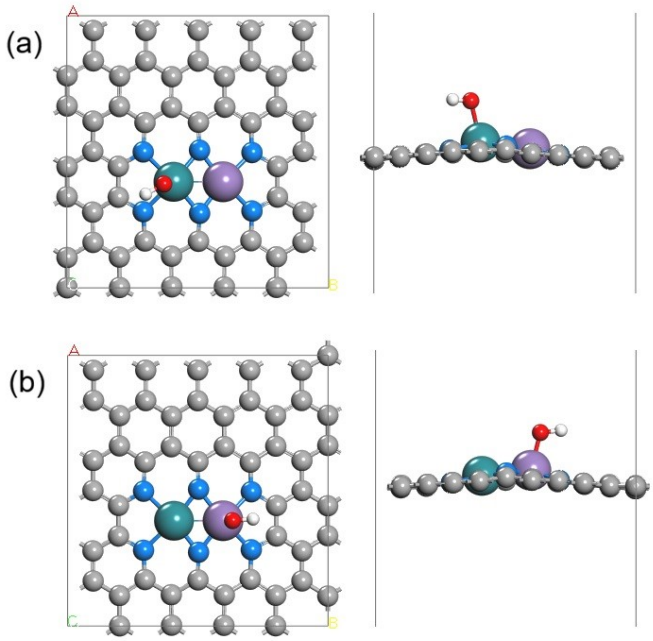

Figure S11 The optimized structures of $^*OH$ on (a) Ru site and (b) Mn site of RuMn-N_6-C_{10}.

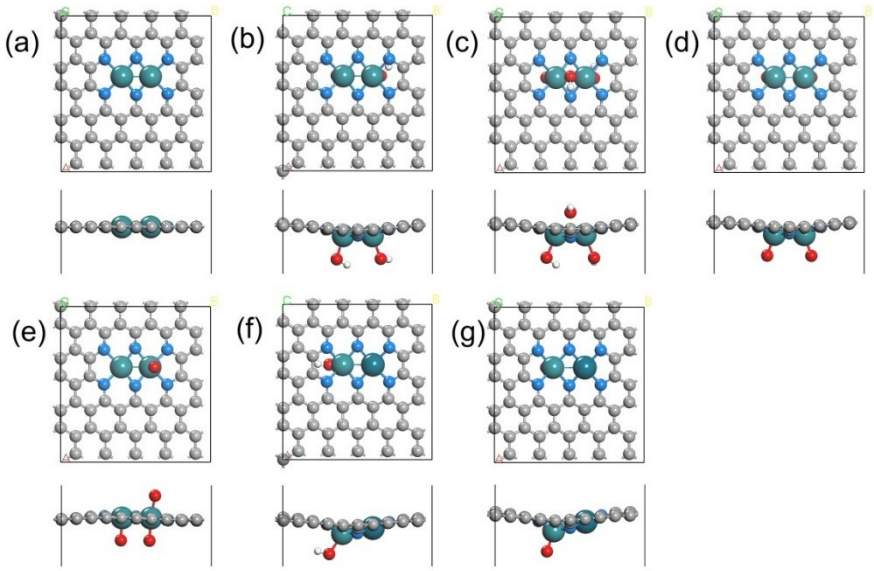

Figure S12 The optimized structures of (a) RuRu-NC, (b) RuRu-O1, (c) RuRu-O2, (d) RuRu-O3, (e) RuRu-O4, (f) RuIr-O1R and (g) RuIr-O3R.

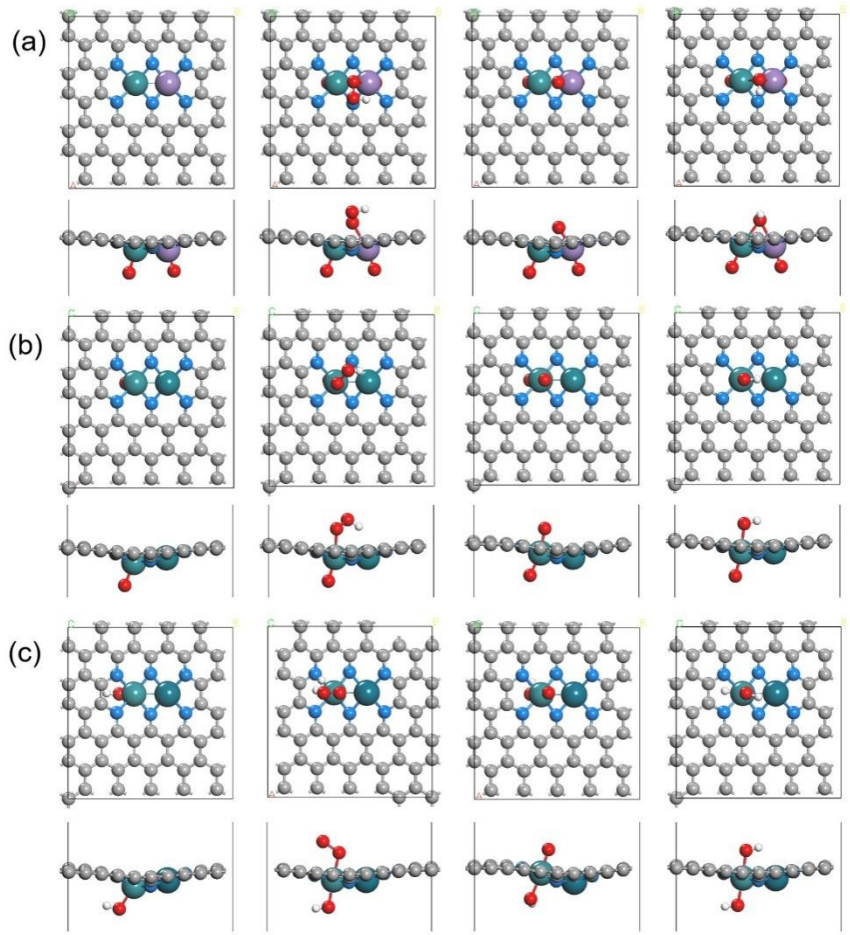

Figure S13 The optimized structures of *OOH, *O and *OH on (a) RuMn-NC-O3, (b) RuRh-NC-O3R and (c) RuPd-NC-O3R.

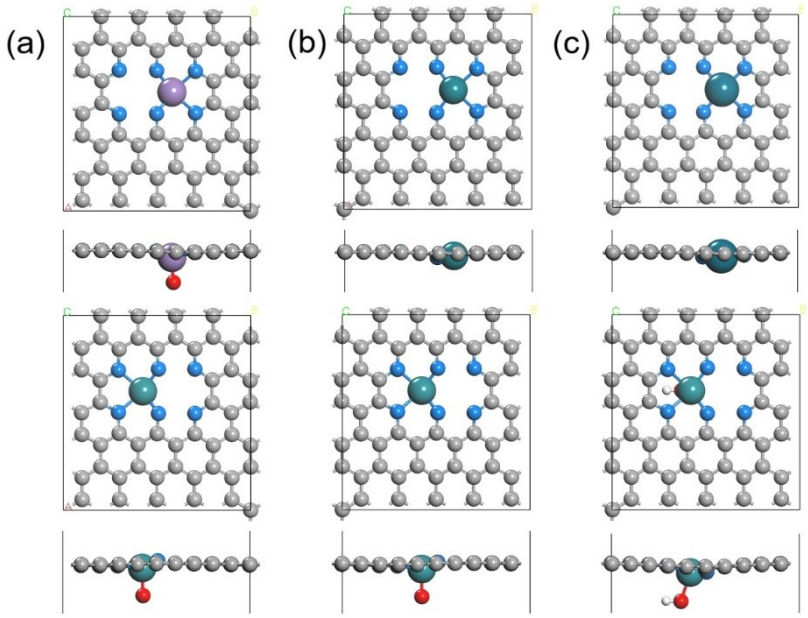

Figure S14 The optimized structures of (a) RuMn-NC-O3, (b) RuRh-NC-O1R, (c) RuPd-NC-O1R with removed Ru^x and M^x.

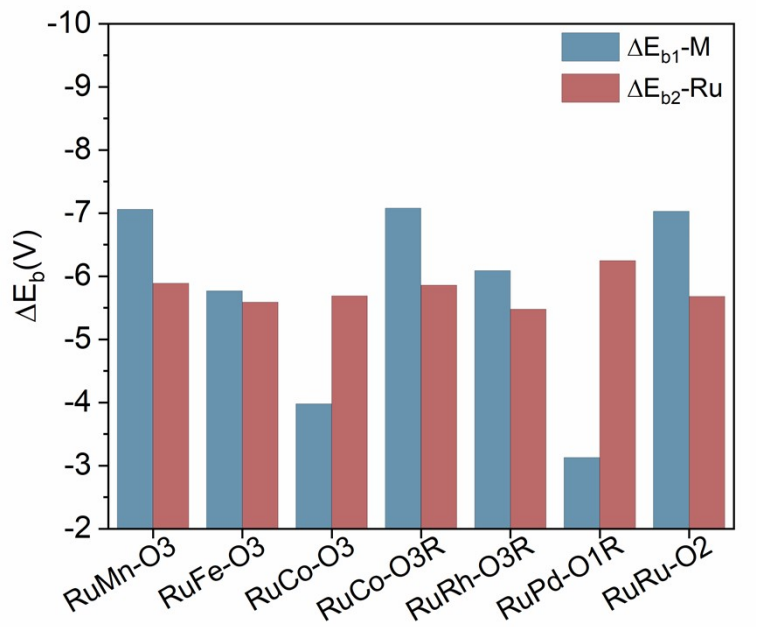

Figure S15 The binding energy comparison of RhMn-NC-O3, RuFe-NC-O3, RuCo-NC-O3, RuCo-NC-O3R, RuRh-NC-O3R, RuPd-NC-O1R, RuRu-NC-O2.

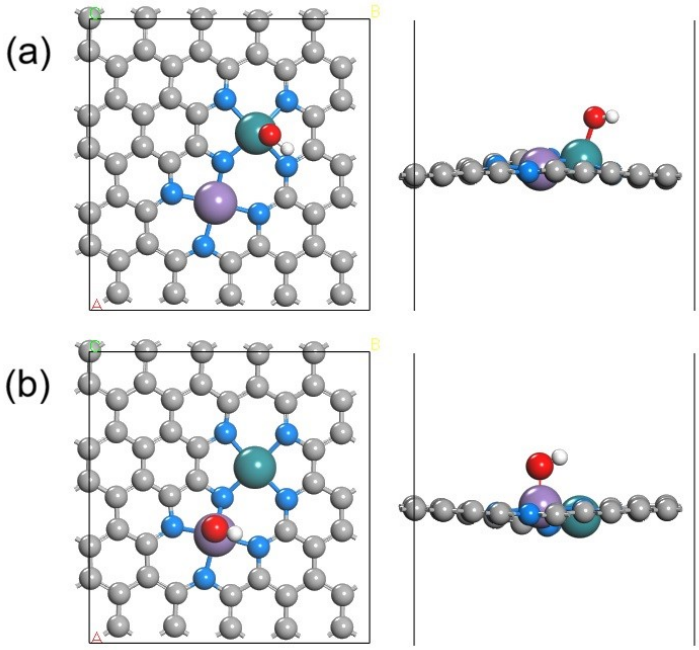

Figure S16 The optimized structures of *OH on (a) Ru site and (b) Mn site of RuN_4-MnN_4.

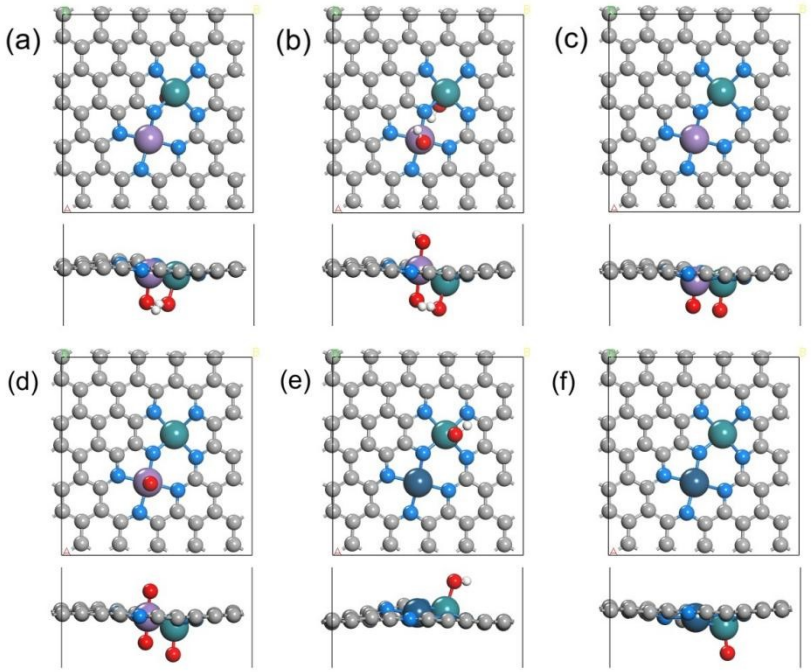

Figure S17 The optimized structures of (a) RuMn-O1, (b) RuMn-O2, (c) RuMn-O3, (d) RuMn-O4, (e) RuMn-O1R, (f) RuMn-O3R.

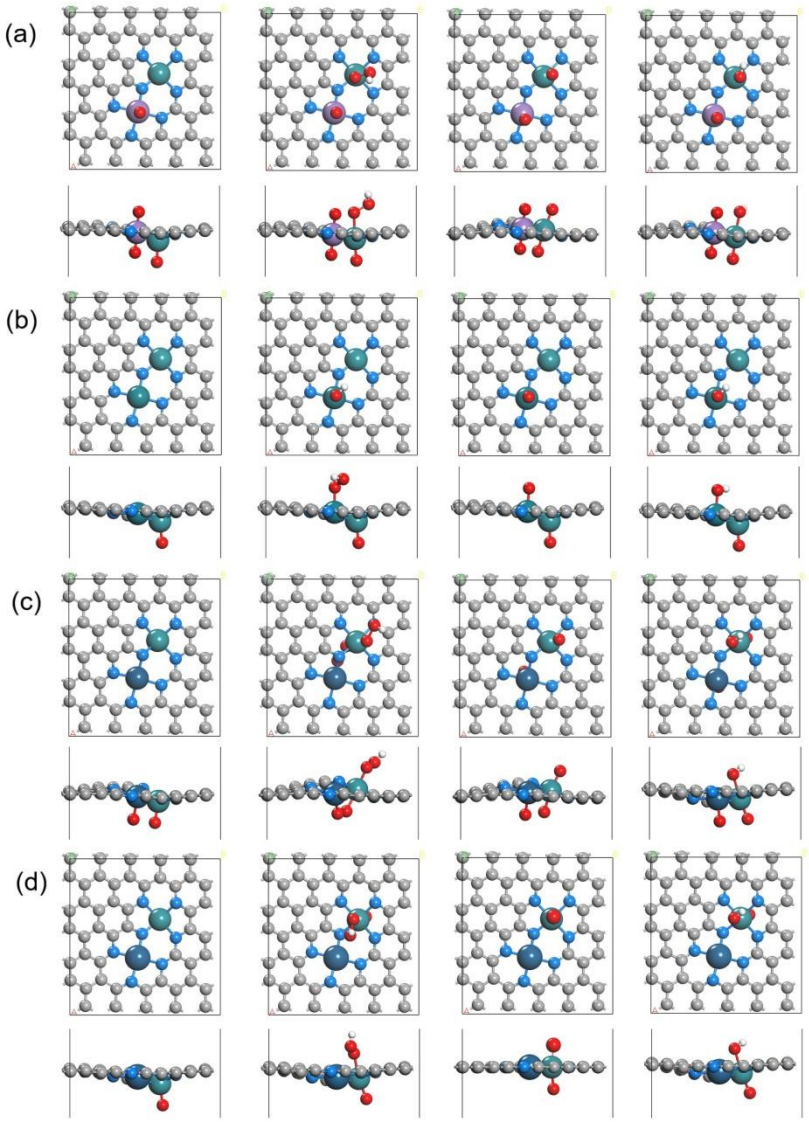

Figure S18 The optimized structures of *OOH, *O and *OH on (a) RuMn-O4, (b) RuRh-O3R(Rh), (c) RuIr-O3 and (d) RuPt-O3R.

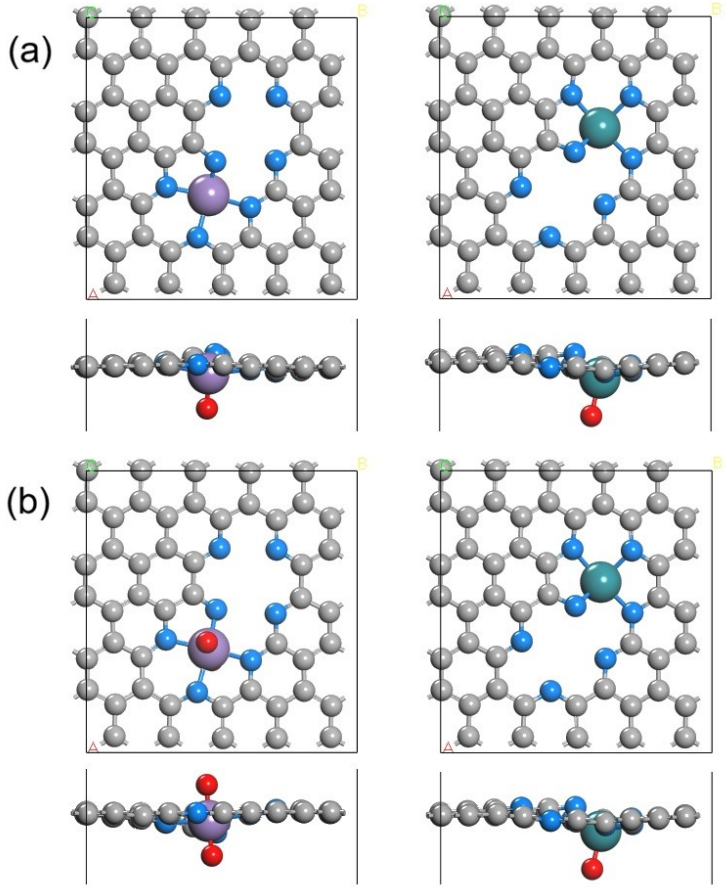

Figure S19 The optimized structures of (a) RuMn-O3 and (b) RuMn-NC-O4 with removed Ru^x and Mn^x.

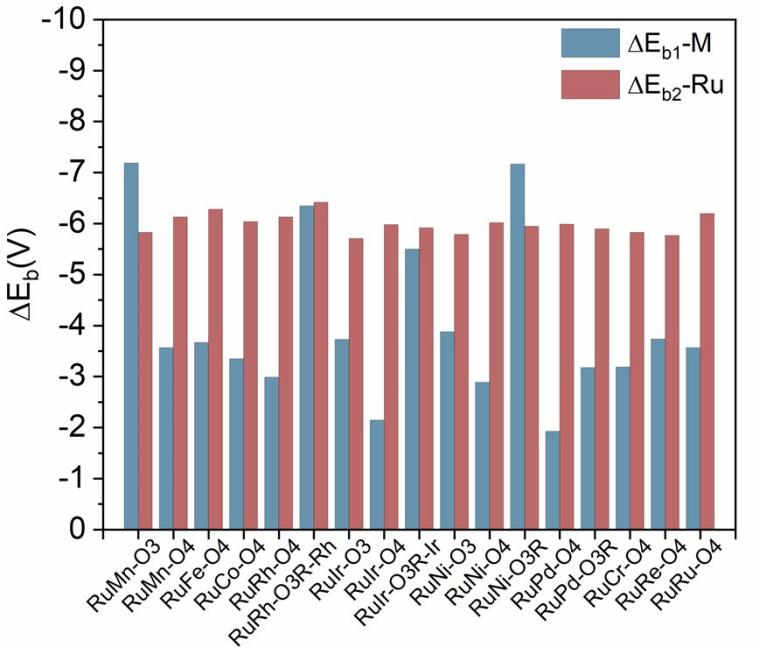

Figure S20 The binding energy comparison of RhM-On.

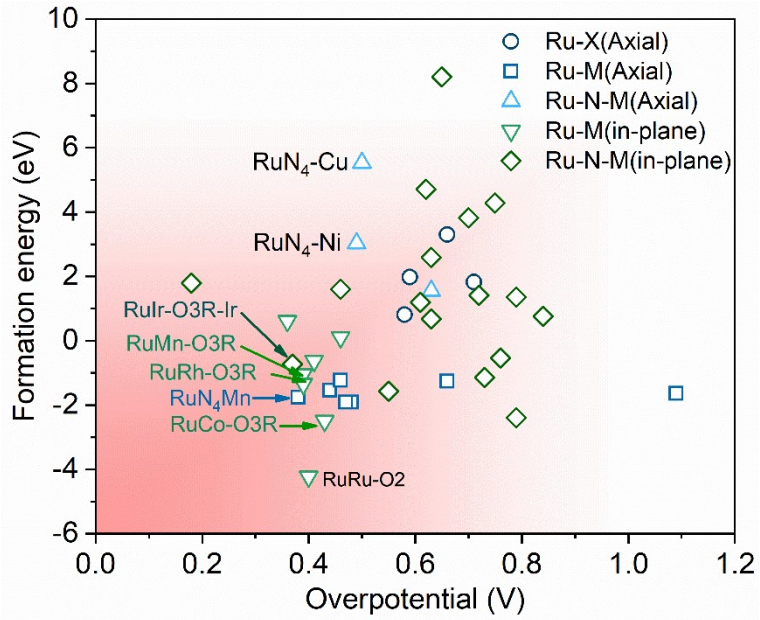

Figure S21. Overpotential vs. formation energy for various Ru-based catalysts

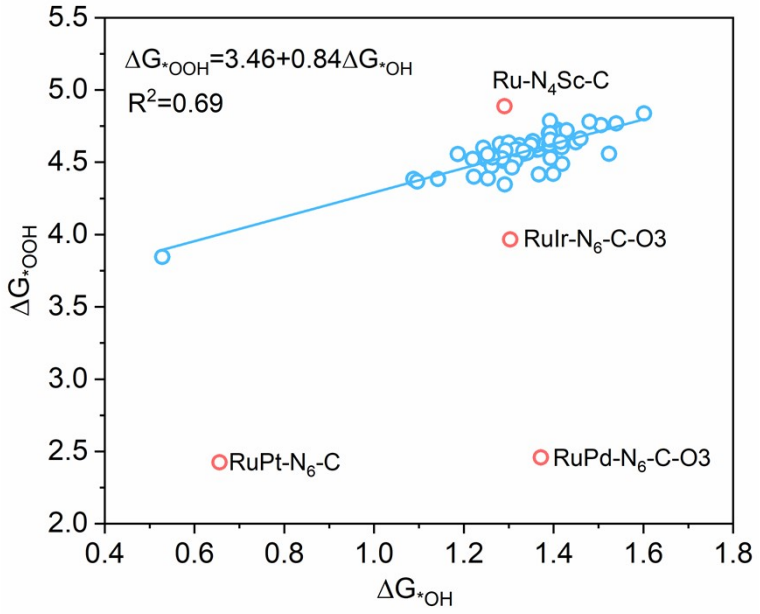

Figure S22. Linear relationship between ΔG_{*OOH} and ΔG_{*OH} for representative Ru-based catalysts

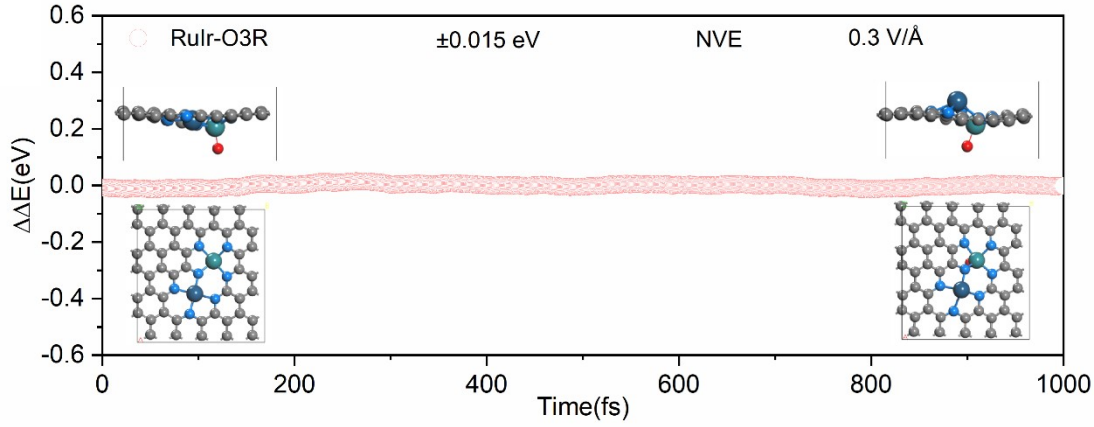

Figure S23. Dynamic stability of RuIr-O3R from AIMD simulations

Table S1. The zero point energies and entropic corrections of oxygenates at 298.15 K

Species	ZPE[a]	TS[a]	ZPE[b]	TS[b]	ZPE[c]	TS[c]	ZPE[d]	TS[d]
O*	0.07	0.00	0.05	0.00	0.084	0.05	0.07	0.05
OH*	0.36	0.00	0.36	0.06	0.386	0.07	0.36	0.11
OOH*	0.39	0.00	0.40	0.08	0.457	0.16	0.45	0.18
O_2	-	-	0.11	0.64	-	-	-	-
H_2	0.27	0.41	0.27	0.41	0.27	0.41	0.27	0.41
H_2O	0.56	0.67	0.56	0.67	0.56	0.67	0.56	0.67

[a]Ling, Chongyi, et al. "Nanosheet Supported Single-Metal Atom Bifunctional Catalyst for Overall Water Splitting." *Nano Letters* 17.8 (2017): 5133-5139.

[b]Zhou, Si, et al. "Nitrogen doped graphene on transition metal substrates as efficient bifunctional catalysts for oxygen reduction and oxygen evolution reactions." *ACS Applied Materials & Interfaces* 9.27 (2017): 22578-22587.

[c]Li, Mingtao, et al. "N-doped graphene as catalysts for oxygen reduction and oxygen evolution reactions: Theoretical considerations." *Journal of Catalysis* 314 (2014): 66-72.

[d]The present work.